Nitrile rubber–bentonite composites: a thermal degradation study

**C. Albano · B. Rodríguez · A. Karam ·
M. Hernández · M. Ichazo · J. González · M. Covis**

Abstract   The aim of the present work was to study the kinetics of the thermal degradation mechanisms of NBR–bentonite composites by means of three methods: E2 Function, Coast-Redfern, and Invariant Kinetics Parameters (IKP). Composites with 10, 20, and 30 phr of pristine bentonite and of treated bentonite with octadecylamine were prepared. Thermogravimetric analysis was followed at different heating rates (5, 7, 10, and 13 °C/min) under N_2 atmosphere. The kinetic parameters values calculated according to the E_2 Function reflect a decrease in the activation energy with the increase in the filler content, being this effect more pronounced for the treated filler, as an indicative of a lower thermal stability. With respect to the IKP method, the activation energy of the different composites lies between 262 and 293 kJ/mol. The distribution of probabilities associated to the 18 kinetic functions indicate that all the studied systems present the kinetic model of nucleation and nuclei growth as the most probable degradation mechanism, S3 with 24% of probability and S1, S2, and S4 with 12%; followed by the interphase reaction model with the S6, S7, and S8 functions with a probability ranging between 13 and 10%. In addition, we can conclude that both types of bentonites employed in this study promote an increase in the probability of the diffusion mechanism, being this fact an indicative of the formation of small molecules that diffuse in the interphase and give rise to degradation mechanisms corresponding to the reaction order kinetic model. Finally, we can say that the results of the thermal study can be corroborated by the rheological behavior and the morphology of the NBR–bentonite composites.

C. Albano (✉) · M. Covis
Facultad de Ingeniería, Escuela de Ingeniería Química, Universidad Central de Venezuela, Caracas, Venezuela
e-mail: carmen.albano@ucv.ve

C. Albano · B. Rodríguez · A. Karam
Laboratorio de Polímeros, Centro de Química, IVIC, Caracas, Venezuela

M. Hernández · M. Ichazo · J. González
Departamento de Mecánica, Universidad Simón Bolívar, Caracas, Venezuela

Introduction

During the last decades, new technologies for obtaining products of better quality and lower cost have emerged. The addition of reinforcing fillers to elastomeric matrices is a clear example of such technologies, by which tensile properties and abrasion resistance can be enhanced. Carbon black has been recognized as the main filler for reinforcing elastomeric vulcanizates; nonetheless, "white" and nanometric size fillers have drawn the attention of many researchers and industries as possible substitutes of carbon black. Among these fillers we can cite clay silicates, such as montmorrillonite, hectorite, bentonite, etc. [1]. These inorganic fillers can be chemically treated in order to improve their interaction with the elastomeric matrix. Examples of these treatments have been reported by López-Manchado et al. [2, 3] in composites of natural rubber and clay treated with bis(trietoxisililpropil)tetrasulfur (TESPT) and by Jin-tae et al. [4] in composites based on nitrile rubber (NBR) and organophilic silicates. In particular, composites based on NBR and organically treated bentonites have been studied by the authors of this research and reported elsewhere [5]. NBR composites have an increasing interest in the petrochemical industry due to their elevated resistance to solvents and chemicals and their improved mechanical performance.

On the other hand, it is known that the study of the thermal decomposition of polymers has been developed by the use of mathematical methods which simulate theoretical models on the kinetics of degradation of the materials. Up to date, the developed methods let us determine approximate values of the kinetic parameters such as the pre-exponential Arrhenius factor and the activation energy, as a function of the mass conversion degree through isothermal or non-isothermal experiments. Among the non-isothermal mathematical models used for the determination of the degradation mechanism of polymeric samples we can cite the E2 Function [6], the Coast-Redfern [7, 8], and the Invariant Kinetics Parameters (IKP) [9] models.

Thus, it is the aim of the present work to study the thermal stability and the thermal degradation mechanisms of vulcanized NBR–bentonite composites by means of three methods: E2 Function, Coast-Redfern, and IKP. The application of these models to the thermogravimetric data obtained from the decomposition of NBR–bentonite samples can let us analyze the thermal stability of the elastomeric matrix, and the influence of the filler content, as well as the influence of the filler surface treatment, on the degradation mechanism of NBR.

Experimental part

Filler treatment

Bentonite (B) was modified by introducing organic ions into the interlayer spacing rendering hydrophobic surfaces via ion exchange reaction. This ion exchange

produces organophilic clays which are more compatible with the polymer [10]. The treatment of the bentonite was done through stirring in aqueous solution with octadecylamine and HCl at 500 rpm and 80 °C. After 1 h at this temperature and under vigorous stirring, the suspension was filtered and dried at 80 °C during 48 h. The dried organoclay (BT) was grinded in a ball mill. Particle size distribution was determined by laser diffraction techniques (Malvern, Mastersizer 2000). Also, the bentonite particles with and without octadecylamine were analyzed and characterized by means of scanning electron microscopy (SEM, Hitachi S-2400) and Fourier Infrared Spectroscopy (FTIR).

Preparation of NBR–bentonite composites

Composites consisting of a *KRYNAC* acrylonitrile-butadiene rubber (NBR) and 10, 20, and 30 phr of *OPTIBENT CP* sodium bentonite were prepared. The samples are referred as NBR*xy*, where *x* and *y* correspond to the amount and type of clay, respectively. Additives for all formulations based on 100 parts of rubber (phr) were: 3 phr of zinc oxide (ZnO) and 1 phr of stearic acid used as the activation complex, 0.7 phr of *N-t*-butyl benzothiazole sulfenamide (TBBS) used as the accelerator and 1.5 phr of sulfur (S) used as the vulcanizing agent. All composites were prepared using a Banbury® internal mixer at a rotor speed of 60 rpm, following the mixing procedure reflected on the ASTM D3568 standard. Curing characteristics were studied using a rotorless rheometer (Ektron Tek EKT-2.00SP) at 170 °C with an oscillation of 0.5° according to the ASTM D5289 procedure.

Characterization of NBR–bentonite composites

Morphology of blends was analyzed by means of SEM and reported elsewhere [5]. Thermogravimetric curves were obtained using a thermal analyzer (Mettler-Toledo TGA/STDA851), under the following conditions: samples of 3–5 mg were heated up to 800 °C under nitrogen atmosphere at different heating rates $\beta = 3, 5, 7, 10,$ and 13 °C/min. Thermogravimetric data was used to calculate the kinetic parameters using the methods E_2 Function, Coast-Redfern, and IKP [6–9].

Theoretical background

During the study of decomposition kinetics of polymers, reactions are considered irreversible and the decomposition rate of the solid depends on temperature and amount of material [11]. If only one type of reaction is involved in the process, it is assumed that the functions can be separated and that the equation used for describing the progress of the reaction can be:

$$\frac{d\alpha}{dt} = k(T)f(\alpha) \tag{1}$$

where t is the time, T is the absolute temperature in (K) and α the degree of transformation defined as:

$$\alpha = \omega^0 - \omega / \omega^0 - \omega^{00} \tag{2}$$

where ω is the mass of the solid and the superscripts 0 and 00 indicate the initial and the remnant mass, respectively.

The function $f(\alpha)$ is related to the reaction mechanism and the rate constant k is expressed by the Arrhenius equation:

$$k = A \exp\left(\frac{-E}{RT}\right) \tag{3}$$

where E is the activation energy, A is the Arrhenius pre-exponential factor, and R the gas constant [12]. When the progress of the reaction and the Arrhenius equation are combined, the following basic expression can be obtained:

$$\frac{d\alpha}{dt} = Af(\alpha)e^{\left(-\frac{E}{RT}\right)} \tag{4}$$

Different methods can be developed with this basic expression in order to evaluate the activation energy. Besides, the parameters can be calculated through experimental dynamic curves, employing as main factors the concentration of reactants and products [13].

Coast-Redfern method

This is an integral method applied to thermogravimetric data in which the reaction orders are assumed to be equal or different to 1, justified by most of the decompositions in solid state. The Coast-Redfern equations are given below [7]:

For $n \neq 1$

$$\log(g(\alpha)) = \log\left[1 - (1-\alpha)^{1-n}\big/T^2(1-n)\right] = \log\frac{AR}{BE}\left(1 - \frac{2RT}{E}\right) - \frac{E}{2.3RT} \tag{5}$$
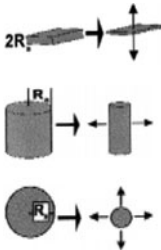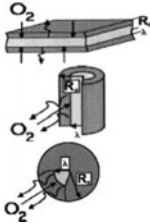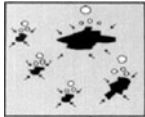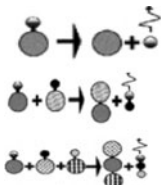
For $n = 1$

$$\log\left(\frac{-\log(1-\alpha)}{T^2}\right) = \log\frac{AR}{BE}\left(1 - \frac{2RT}{E}\right) - \frac{E}{2.3RT} \tag{6}$$

These equations can be applied to different $g(\alpha)$ functions that describe 18 possible decomposition mechanisms. Table 1 compiles all the different functions [14]. When representing the left part of Eq. 6 for different values of α, as a function of reciprocal temperature, a linear correlation can be defined where the slope and the intercept let us obtain the activation energy and the pre-exponential factor, respectively [15].

E_2 Function method

This is an integral method that allows the calculation of the activation energy once the reaction order and three conversions are known with their respective temperatures. The reaction order is obtained by the application of the Coast-Redfern [7] method and usually applied conversions correspond to 5, 50, and 95% of mass of the sample. The equations used for the E_2 Function are [16]:

Table 1 Degradation functions employed in the calculus methods [9]

Kinetic model	$f_{j\alpha}$	$g_{j\alpha}$/Parameter S	Visualization of the physical phenomenon
Nucleation and nuclei growth	$(1-\alpha)(-\ln(1-\alpha))^{1-n}$	$(-\ln(1-\alpha))^n$ S1, $n = 1/4$; S2, $n = 1/3$; S3, $n = 1/2$; S4, $n = 2/3$	
Reaction in the phase limit	$(1-\alpha)^n$	$1-(1-\alpha)$ S6, planar symmetry; $2[1-(1-\alpha)^{1/2}]$ S7, cylindrical symmetry; $3[1-(1-\alpha)^{1/3}]$ S8, spherical symmetry	
Diffusion	$1/2\alpha^{-1}$; $(-\ln(1-\alpha))^{-1}$	α^2 S9, planar symmetry; $(1-\alpha)\ln(1-\alpha)-\alpha$ S10 cylindrical symmetry	
	$3/2\,[(1-\alpha)^{-1/3}-1]^{-1}$; $3/2(1-\alpha)^{1/3}[(1-\alpha)^{-1/3}-1]^{-1}$	$1-2/3\alpha-(1-\alpha)^{2/3}$ S11 spherical symmetry; $[(1-\alpha)^{1/3}-1]^2$ S18, Jander type	
Potential law	$(1/n)\alpha^{1-n}$	α^n $(0 < n < 2)$ S12, $n = 1/4$; S13, $n = 1/3$; S14, $n = 1/2$; S17, $n = 3/2$	
Reaction order	$(1-\alpha)$; $(1/n)(1-\alpha)^{1-n}$	$-\ln(1-\alpha)$ S5, $n = 1$; $1-(1-\alpha)^{1/2}$ S15, $n = 1/2$; $1-(1-\alpha)^{1/3}$ S16, $n = 1/3$	

For $n \neq 1$

$$\frac{(1-\alpha_1)^{1-n}-(1-\alpha_2)^{1-n}}{(1-\alpha_2)^{1-n}-(1-\alpha_3)^{1-n}} = \frac{T_2 E_2\left(\frac{E}{RT_2}\right) - T_1 E_2\left(\frac{E}{RT_1}\right)}{T_3 E_2\left(\frac{E}{RT_3}\right) - T_2 E_2\left(\frac{E}{RT_2}\right)} \tag{7}$$

For $n = 1$

$$\frac{\ln\left[\frac{(1-\alpha_1)}{(1-\alpha_2)}\right]}{\ln\left[\frac{(1-\alpha_2)}{(1-\alpha_3)}\right]} = \frac{T_2 E_2\left(\frac{E}{RT_2}\right) - T_1 E_2\left(\frac{E}{RT_1}\right)}{T_3 E_2\left(\frac{E}{RT_3}\right) - T_2 E_2\left(\frac{E}{RT_2}\right)} \quad (8)$$

IKP method

The IKP model is based on the study of the thermogravimetric data obtained at different rates. If compared to classical methods such as Coast-Redfern [7, 8], Horowitz-Metzgar [16], or Friedman [17], this method has the advantage of making no suppositions on the degradation kinetics and that results are independent on experimental conditions [18]. One experimental curve $\alpha = \alpha(T)$ can be described by various conversion functions and by one simple thermogravimetric curve, the activation parameters can be calculated for the different $f(\alpha)$ functions corresponding to the 18 possible degradation mechanisms (Table 1), which are related by the *compensation effect*. At each heating rate β_v, the pairs (A_{vj}, E_{vj}) characteristic for each conversion function are determined by using an integral method such as the Coast-Redfern Method. The application of the compensation effect allows us to obtain the compensation parameters (α_v^*, β_v^*) for each heating rate. The intersection of the linear graph $\ln A_v$ vs. E_v for different heating rates corresponds to the true A and E parameters, defined by Lesnikovich [19] as invariant activation parameters (A_{inv}, E_{inv}). The evaluation of these invariant parameters is calculated by use of the following equation:

$$\ln A_{inv} = \alpha_v^* + \beta_v^* E_{inv} \quad (9)$$

where α_v^* vs. β_v^* is a straight line that permits the evaluation of the invariant parameters [9, 14].

Results and discussion

Filler characterization

The chemical and thermal characterization of both fillers, treated bentonite (BT) and pristine bentonite (B), is an important issue for establishing differences in the prepared NBR composites. Previous results of this characterization are published elsewhere [5].

As a summary, we can say that from the particle size distribution the treated bentonite shows a smaller particle size (36.7 μm) and that the particles tend to agglomerate regardless the nature of the clay. From the XRD patterns, we can confirm that the treated clay has a well-delaminated structure, and from the peaks present in the FTIR spectra, there is evidence that the treated clay presents a hydrophobic nature and that the ammonium salt has been properly incorporated within the silicate layers [5].

Table 2 Decomposition temperatures of bentonite

Filler	T_{id} (°C)	T_{fd} (°C)
Pristine bentonite (B)	377.5	482.9
Treated bentonite (BT)	188.5	719.9

In order to complete the characterization of the filler, a thermogravimetric analysis was performed at 10 °C/min under a nitrogen atmosphere. Results show that the thermal decomposition process takes place in two steps; the first one corresponds to the water loss and the second one to the decomposition of the clay samples. Treated bentonite shows an initial decomposition temperature (T_{id}) 189 °C lower than that of the pristine bentonite (see Table 2). This fact is an evidence of the organoamines present in the BT, since it is known that this kind of organomodifiers start to decompose around 200 °C, thus reducing the thermal stability of the clay [20]. In addition, we can see that BT finishes its decomposition process (T_{fd}) at a higher temperature than that observed for the pristine clay.

Thermogravimetric analysis: determination of kinetic parameters

Figure 1 shows the thermograms of neat NBR (NBR00) and of the NBR composites with 20 phr of both bentonites (B and BT). The analysis of such curves reflects that the decomposition process of all samples, under a N_2 atmosphere and at different heating rates occurs in only one step. In addition, one can see that the T_{id} of the composites decreases in presence of the filler and remains invariable with the filler content. Nonetheless, this behavior is not reflected by the final decomposition temperatures (T_{fd}) since they do not show significant variations as shown in Table 3.

In addition, all composites show remnant mass percentages depending on the decomposition process of the elastomer as well as on the filler content; this fact can be attributed to the heterogeneity of the composites (see Table 4). The elastomer without filler (NBR00) showed remaining mass percentages between 8 and 9% due to the probably of crosslinking reactions produced during the degradation process, also this remaining mass contains the contribution of the additives used in the process of vulcanization of the elastomer. Additionally, the synthetic rubber (NBR) decomposition was produced by random-chain scission with intramolecular hydrogen transfer producing a weight loss above 90% [21, 22].

On the other hand, samples with 10% of filler, treated (BT) or pristine (B) showed about 16% of remaining mass, of which 10% correspond to the added filler and additional 6% to crosslinking processes of the elastomer and other additives. These data was obtained by difference between the final and initial mass, for samples NBR00 and NBR10B, from thermograms carried out at different heating rates. The increment in the remanent mass percentage was attributed to the filler.

Moreover, NBR20B and NBR20BT formulations showed about 22% of remaining mass that correspond to the filler added. By contrast, samples with 30% of B and BT showed about 25% of remnant mass, this value is lower than expected. This could be attributed to heterogeneity of these compounds because of high levels of filler due to formation of agglomerates [22].
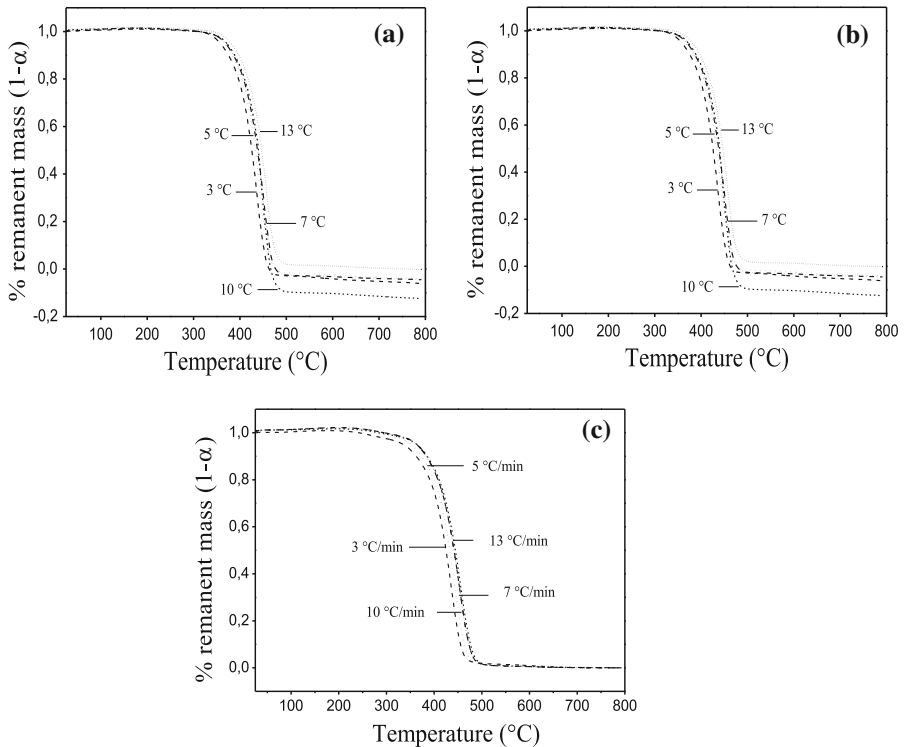
Fig. 1 Decomposition thermograms of composites: **a** neat NBR, **b** NBR20B, **c** NBR20BT at different reaction rates

Table 3 Decomposition temperatures of NBR–bentonite composites at different heating rates (T_{id} and T_{fd}: initial and final decomposition temperatures)

Composite	Heating rate (°C/min)									
	3		5		7		10		13	
Decomposition temperature (°C):	T_{id}	T_{fd}	T_{id}	T_{fd}	T_{id}	T_{fd}	T_{id}	T_{fd}	T_{id}	T_{fd}
NBR00	412	462	440	474	410	476	422	477	410	485
NBR10B	387	465	396	477	406	481	397	489	409	488
NBR20B	394	467	416	474	395	481	395	489	396	493
NBR30B	395	465	399	475	389	481	396	487	395	493
NBR10BT	395	467	387	476	390	482	392	488	392	492
NBR20BT	388	468	390	478	391	484	391	489	394	493
NBR30BT	388	466	387	477	488	483	387	489	388	493

The activation energy (E) calculated according to the E_2 Function method for neat NBR was 238.03 kJ/mol for a heating rate of 3 °C/min. This value was maintained for the five heating rates in the range of 238–245 kJ/mol (Table 5), in accordance with reported data [23]. We can also observe that for the filled samples,

Table 4 Remnant mass of the decomposition of NBR–bentonite composites at different heating rates

Composite	% Remnant mass				
	Heating rate (°C/min)				
	3	5	7	10	13
NBR00	9.2	8.7	8.5	9.1	8.2
NBR10B	16.9	13.0	15.8	16.6	15.1
NBR20B	22.8	21.6	21.8	21.2	20.8
NBR30B	24.7	23.4	26.9	25.8	25.8
NBR10BT	16.0	15.6	15.6	15.6	15.5
NBR20BT	22.3	22.1	22.1	22.1	20.8
NBR30BT	24.7	26.3	25.3	25.3	25.2

Table 5 Kinetic parameters (KP) according to the E_2 Function method for the NBR–bentonite composites. (E: kJ/mol, A: l/min) at different heating rate (HR: (°C/min))

HR	KP	NBR00	NBR 10B	NBR 20B	NBR 30B	NBR 10BT	NBR 20BT	NBR 30BT
3	E	238	209	206	210	204	193	73
	A	2.3×10^{18}	1.7×10^{16}	8.5×10^{15}	1.7×10^{16}	5.7×10^{15}	9.0×10^{14}	1.9×10^{8}
5	E	243	198	212	208	197	189	69
	A	5.9×10^{18}	2.2×10^{15}	2.8×10^{16}	1.3×10^{16}	2.0×10^{15}	4.9×10^{14}	7.0×10^{8}
7	E	245	204	194	194	194	185	68
	A	8.6×10^{18}	8.1×10^{15}	1.4×10^{15}	1.3×10^{15}	1.2×10^{15}	2.5×10^{14}	5.7×10^{8}
10	E	237	189	192	192	189	182	67
	A	3.2×10^{18}	5.9×10^{14}	9.6×10^{14}	1.0×10^{15}	6.2×10^{14}	1.9×10^{14}	5.1×10^{8}
13	E	235	215	190	187	186	179	66
	A	1.9×10^{18}	6.7×10^{16}	8.2×10^{14}	4.6×10^{14}	4.4×10^{14}	1.2×10^{14}	4.5×10^{8}

as filler content increases the activation energy of the elastomeric matrix shows a gradual decrease, thus reducing the thermal stability of the composites. This behavior is more drastic for the composites filled with the treated clay. A schematic representation of the thermal degradation mechanism of the NBR–bentonite composites is shown in Fig. 2 [24].

When the material is heated, different process occur in both phases, the gaseous and the condensed phase; these processes depend on factors such as mass and heat transfer, which vary with the type of matrix, and are also strongly influenced by the type of degradation suffered by the material, and by the nature and surface treatment of the filler (see Fig. 3).

Clay modifiers with multiple branching present higher thermal stability if compared to those formed by single chains [20]. In this study the modifying agent of the filler is a linear alkyl amine, whose behavior is similar to surfactants since it is formed by a hydrophobic tail and a hydrophilic head, an alkyl chain of 18 carbons
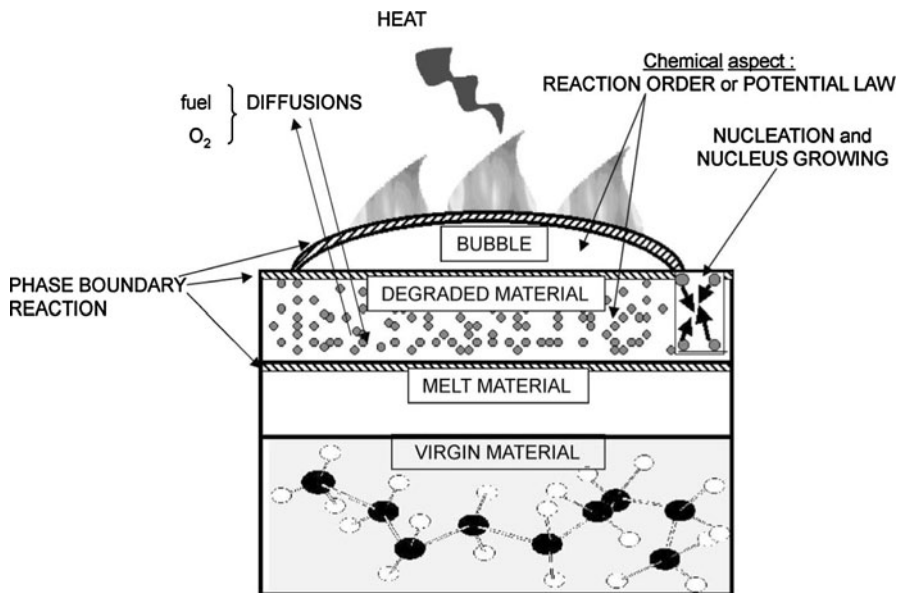
Fig. 2 Schematic representation of the thermal degradation mechanism of the polymeric materials [24]

and an amine functional group, respectively. Such modifier could promote a decrease on the thermal stability of the rubber by means of the degradation reactions reported for alkyl surfactants [25]. In fact, pyrolysis studies of organo-layered silicates have indicated that the thermal decomposition of the ammonium surfactant in the clay interlayer generally proceeds by Hoffmann elimination process. This reaction yields an amine, an olefin, and an acidic site on layered silicate (see Fig. 3). Additionally, the 1-chloroalkanes are typical decomposition products of the alkylammonium halides, and their formation occurs through SN2 nucleophilic substitution reaction when there are ammonium surfactant without interaction with clay interlayer (see Fig. 3) [26].

Another kinetic parameter, the Arrhenius pre-exponential factor A, was also evaluated. It can be observed in Table 5 that this parameter decreases when the rubber is filled and that this decrease is of approximately four orders of magnitude for composites filled with up to 30 phr of B and with up to 20 phr of BT. The more significant decrease on the A values (10 orders of magnitude) is obtained when 30 phr of BT are present, being this result in concordance with the lower activation energy values.

The application of the IKP method to the data obtained at 5 heating rates (3, 5, 7, 10, and 13 °C/min) lets us observe the *compensation effect* and lets us calculate the invariant kinetic parameters for all the composites. The determined parameters are listed in Table 6. According to the IKP method, the E values reflect a slight decrease on the thermal stability of the rubbery matrix as filler content increases, regardless of the nature of the filler.
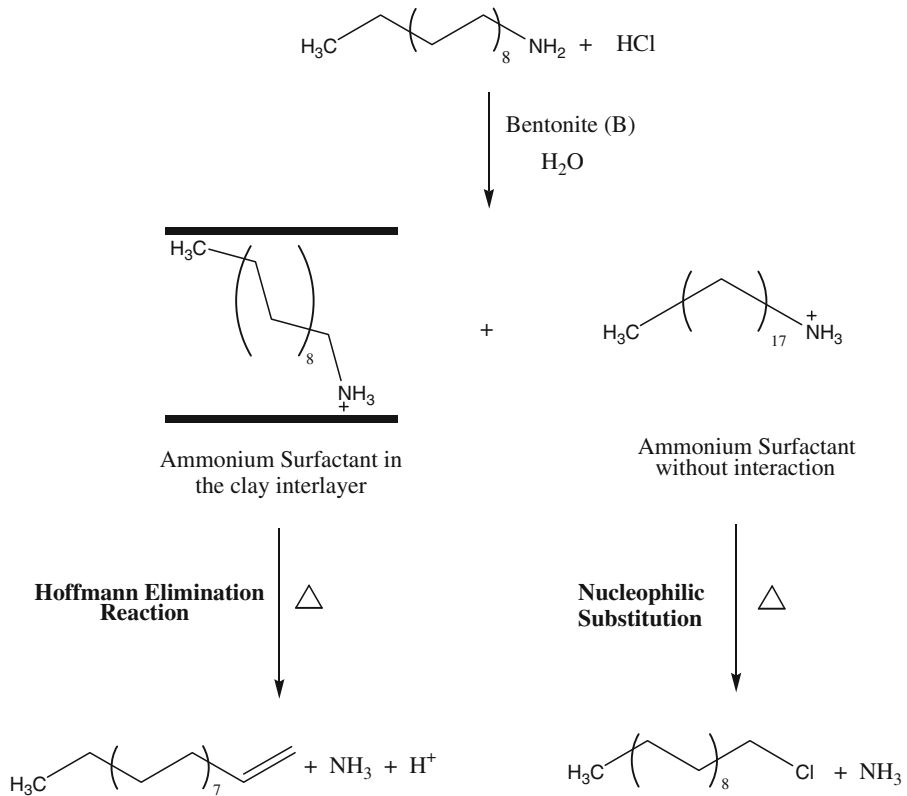
Fig. 3 Decomposition mechanism of organic clay modifiers [26]

Table 6 Invariant kinetic parameters of the NBR–bentonite composites

Composites	E (kJ/mol)	A (l/min)	R^2
NBR00	291.75	1.73×10^{20}	0.8271
NBR10B	271.35	5.16×10^{18}	0.9961
NBR20B	275.02	9.06×10^{18}	0.9996
NBR30B	262.58	1.18×10^{18}	0.8556
NBR10BT	293.83	2.09×10^{20}	0.9959
NBR20BT	288.71	8.63×10^{19}	0.9962
NBR30BT	267.08	2.50×10^{18}	0.9819

The probability distribution of the kinetic degradation functions listed in Table 1 is shown in Fig. 4. These distributions indicate that the degradation processes of higher impact for neat NBR (Fig. 4a) is the kinetic model of nucleation and nuclei growth, being the S3 function corresponding to $n = 1/2$ the one with higher probability (24%), and S1, S2, and S4 with 12%, respectively. Regarding the second most probable model, it corresponds to the interphase reaction with the S6, S7, and S8 functions with a probability ranging between 13 and 10%. With a lower
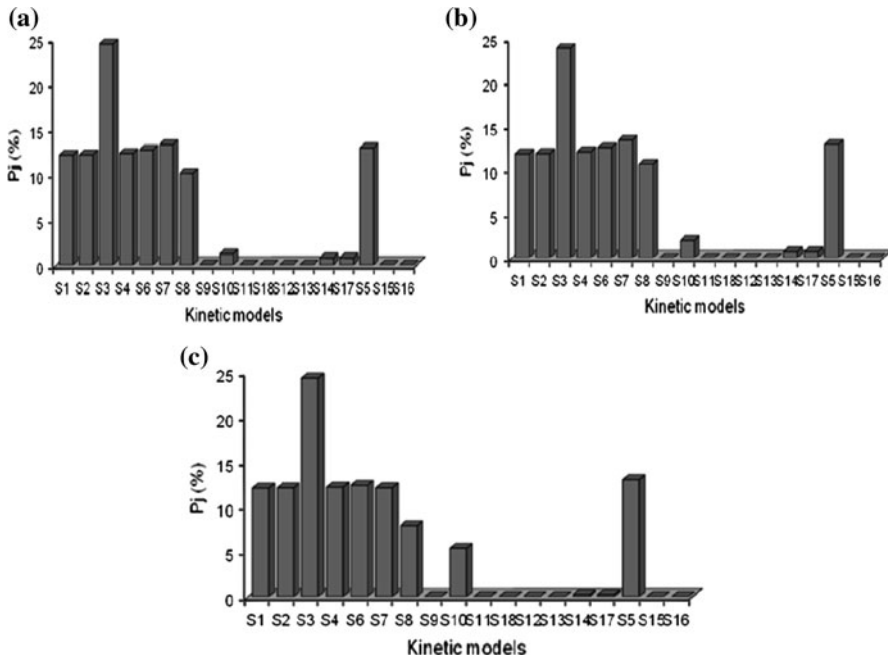
Fig. 4 Probability distribution of the kinetic degradation functions of: **a** NBR00, **b** NBR20B, **c** NBR20BT

participation lies the kinetic model of reaction order (S5 function with 13%) and S4 and S7 corresponding to potential law and reaction order models.

And last, the diffusion mechanism (S10) with less than 1%. With respect to the filled NBR composites, it could be said in general terms that neither the neat clay (B) nor the treated one (BT) affect significantly the mechanisms involved in the degradation process of NBR. However, two facts can be highlighted from the data shown in Fig. 4b and c corresponding to the NBR composites with 20 phr of filler. Firstly, a slight increase from 1 to 3% (NBR20B) and from 1 to 6% (NBR20BT) is observed for the diffusion kinetic model (S10); secondly, S14 and S17 decrease to values around 0%. From these results we can infer that during the global decomposition process of NBR composites, low molecular weight molecules are being produced and diffused through the interphase (model S10) and giving rise to reactions of order 1. So we can say that there is no single degradation mechanism for the studied systems, since it is composed of different processes that give the degradation a heterogeneous nature. In addition, the type of filler added to the elastomeric matrix does not have a notorious impact on the thermal degradation of such systems.

At this point it is worth mentioning that in our previous study concerning the rheometric properties of NBR–bentonite composites [5], we have found that the minimum torque M_L increased by the addition of the clay to the NBR matrix; and that the modification of the bentonite increased even more the viscosity of the
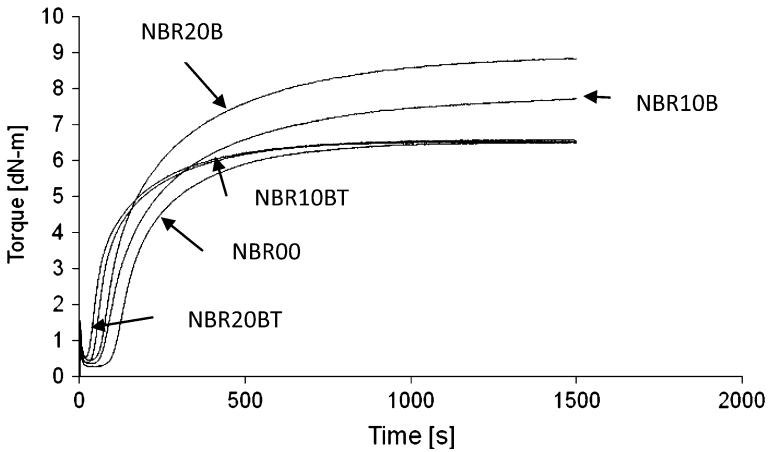
Fig. 5 Rheometric curves obtained at 170 °C for: NBR00, NBR10B, NBR10BT, NBR20B, and NBR20BT

system. The maximum elastic torque M_H values also increased with the presence of the bentonite; nonetheless, the rise in this parameter for the composites with the treated filler was less significant. In general, the presence of fillers restricts deformation, and consequently, the composite become harder and stiffer thereby increasing the torque of the vulcanizates. Other parameters such as scorch time t_{s2} decreased for the composites with the treated clay, probably due to its basic nature; and the time corresponding to 90% of the maximum torque t_{90} increased for the composites with the pristine clay with respect to the value presented for the unfilled NBR.

Figure 5 shows the rheometric curves obtained for the different NBR–bentonite composites. These properties confirm the fact that the modification of the filler has been successfully done and that the octadecylamine has been incorporated within the silicate layers, facilitating the curing reaction due to a decrease in the curve periods observed. Although the initial cured reactions occur faster for the BT samples, it was observed that the final torque was lower in comparison with the NBRB sample. The decrease of this property indicate that the NBRBT composites present a major tendency towards degradation due to the presence of octadecil-amine, since the organoamine produces the thermal decomposition reactions mention above (Fig. 3), these could be acting as possible nuclei initiating the decomposition reactions of the composites.

With respect to the morphology of the NBR composites, the microphotograph shown in Fig. 6a presents the smooth fracture surface of the NBR matrix, while in Fig. 6b, we can clearly see an irregular surface with voids derivatives of the cavitation of the bentonite particles from the elastomeric matrix corresponding to the NBR30B composite. This fact could point out that the untreated bentonite has a poor adhesion with the polymer matrix due to its hydrophilic nature. As a comparison, the morphology of the NBR30BT composite is presented in Fig. 6c. In this case, we can detail a minimum amount of holes, as an indicative of a better
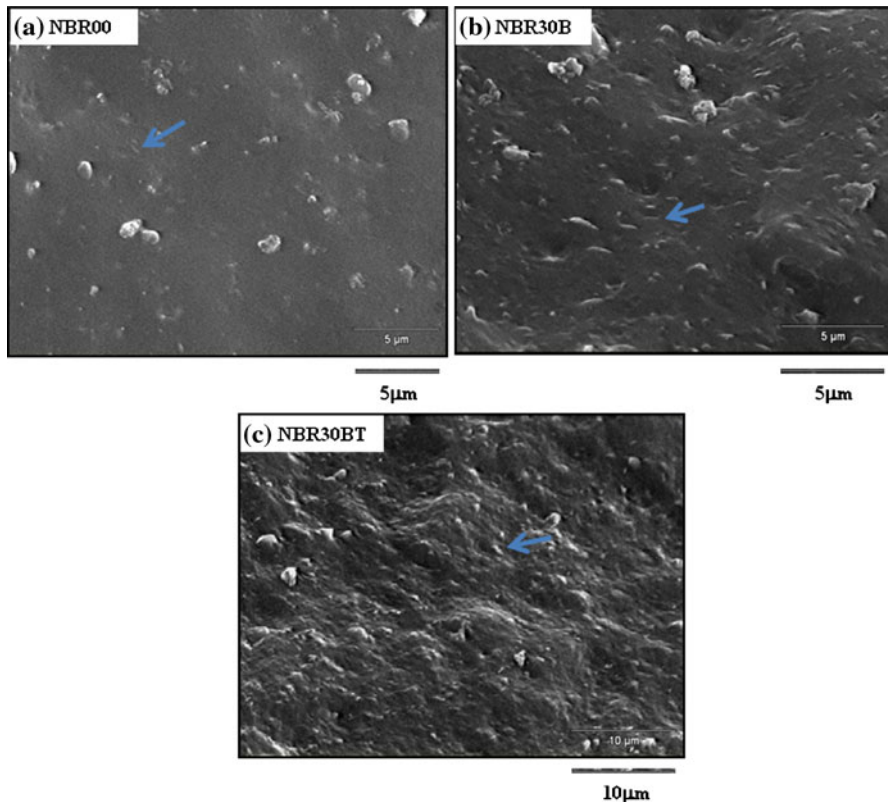
Fig. 6 SEM imagines: **a** NBR00, **b** NBR30B, and **c** NBR30BT

adhesion of the modified clay to the rubber, thus facilitating the interaction between the filler and the NBR matrix. The improved rubber–filler interaction observed by means of SEM for the NBR composites filled with the treated clay reflects the presence of more interaction points between the organic chains intercalated into the filler and the polymeric matrix. Hence, the number of possible initiator sites of the degradation process increases and so the thermal stability of the NBR matrix decreases.

Conclusions

The activation energy calculated according to the E_2 Function and IKP lies in the interval of 235–245 kJ/mol and 291.75 kJ/mol for unfilled NBR, respectively. In both methods, these values decrease slightly as bentonite content increases, regardless of the nature of the clay. In addition, by means of the E2 function method we can conclude that the thermal stability of the rubber matrix decreases drastically in presence of the treated clay, being this fact attributed to the increase in the number of sites that could act as initiators of the degradation reaction. According to

the study of probabilities associated with 18 degradation kinetic functions, we can infer that the pristine clay and the treated clay do not influence significantly the mechanisms involved in the degradation of the NBR, and that the principal kinetic mechanisms are nucleation and nuclei growth, S3 with 24% of probability and S1, S2, and S4 with 12%; and the interphase reaction with the S6, S7, and S8 functions with a probability ranging between 13 and 10%. In addition, we can conclude that both types of bentonites employed in this study promote an increase in the probability of the diffusion mechanism, being this fact an indicative of the formation of small molecules that diffuse in the interphase and give rise to degradation mechanisms corresponding to the reaction order kinetic model. Finally, we can say that the results of the thermal study can be corroborated by the rheological behavior and the morphology of the NBR–bentonite composites.

References

1. Vaia RA, Jandt K, Kramer E, Giannelis EO (1995) Kinetics of polymer melt intercalation. Macromolecules 28:8080
2. López-Manchado M, Herrero B, Arroyo M (2004) Organoclay–natural rubber nanocomposites synthesized by mechanical and solution mixing methods. Polym Int 53:1766–1772
3. López-Manchado M, Herrero B, Biagiotti J (2003) Vulcanization kinetics of natural rubber–organoclay nanocomposites. J Appl Polym Sci 89:1–15
4. Jin-Tae K, Taeg-Su Oh, Dog-ho L (2003) Morphology and rheological properties of nanocomposites based on nitrile rubber and organophilic layered silicates. Polym Int 52(7):1203–1208
5. Albano C, Hernández M, Ichazo M, González J, DeSousa W (2011) Characterization of NBR/bentonite composites: vulcanization kinetics and rheometric and mechanical properties. Polym Bull 67:653–667
6. Chen H, Lin Y, Lai K (2004) Methods for determining the kinetic parameters from nonisothermal thermogravimetry: a comparison of reliability. J Chem Eng Jpn 37:1172–1178
7. Coast AW, Redfern JP (1964) Kinetics parameters from thermogravimetric date. Nature 201:68
8. Coast AW, Redfern JP (1965) Kinetic parameters from thermogravimetric data. II. J Polym Sci Part B Polym Lett 3:917
9. Budrigeac P (2001) Thermal degradation of glass reinforced epoxy resin and polychloroprene rubber: the correlation of kinetic parameters of isothermal accelerated aging with those obtained from non-isothermal data. Polym Degrad Stab 74:125–132
10. Avalos F, Ortiz J, Zitzumbo R, López-Manchado M, Verdejo R, Arroyo M (2008) Effect of montmorillonite intercalant structure on the cure parameters of natural rubber. Eur Polym J 44:3108–3115
11. Albano C, González J, Ichazo I, Kaiser K (1999) Thermal stability of blends of polyolefins and sisal fiber. Polym Degrad Stab 66:179–190
12. Órfao J, Martins F (2002) Kinetic analysis of thermogravimetric data obtained under linear temperature programming—a method based on calculations of the temperature integral by interpolation. Thermochim Acta 390:195–211
13. Albano C, Sanchez G (1999) Study of the mechanical, thermal, and thermodegradative properties of virgin PP with recycled and non-recycled HDPE. Polym Eng Sci 39(8):1456–1461
14. Bourbigot S, Flambard X, Duquesne S (2001) Thermal degradation of poly(p-phenylenebenzobisoxazole) and poly(p-phenylenediamine terephthalamide) fibres. Polym Int 50:157–164
15. Ebrahimi-Kahrizsangi R, Abbasi MH (2008) Evaluation of reliability of Coats-Redfern method for kinetic analysis of non-isothermal TGA. Trans Nonferrous Met Soc China 18:217–221
16. Horowitz HH, Metzger G (1963) A new analysis of thermogravimetric traces. Anal Chem 35:1464
17. Friedman HL (1964) Kinetics of thermal degradation of char-forming plastics from thermogravimetric. Application to a phenolic plastic. J Polym Sci C6:183–195

18. Siat C, Bourbigot S, Le Bras M (1997) Thermal behaviour of polyamide-6-based intumescent formulations—a kinetic study. Polym Degrad Stab 58:303–313

19. Lesnikovich AI, Levchik SV (1983) A method of finding invariant values of kinetics parameters. J Therm Anal 27:83

20. Shah SK, Paul DR (2006) Organoclay degradation in melt processed polyethylene nanocomposites. Polymer 47:4075–4084

21. Rasha MM, Reda M, Mohamed MA, Magdy MK (2010) Electrical and thermal properties of γ-irradiated nitrile rubber/rice husk ash composites. J Appl Polym Sci 115:1495–1502

22. Varkey JT, Augustine S, Thomas S (2000) Thermal degradation of natural rubber/styrene butadiene rubber latex blends by thermogravimetric method. Polym-Plast Technol Eng 39:415–435

23. Namita RC, Anil KB (1996) Thermostable insulating thermoplastic elastomer from rubber polycarbonate blends. J Elast Plast 28:161–181

24. Almera X, Dabrowski F, Le Bras M, Delobel R, Bourbigot S, Marosi G, Anna P (2002) Using polyamide 6 as charring agent in intumescent polypropylene formulations II. Thermal degradation. Polym Degrad Stab 77:315–323

25. Hwu JM, Jiang GJ, Gao ZM, Xie W, Pan WP (2002) The characterization of organic modified clay and clay-filled PMMA nanocomposite. J Appl Polym Sci 83:1702–1710

26. Bertini F, Canetti M, Leone G, Tritto I (2009) Thermal behavior and pyrolysis products of modified organo-layered silicates as intermediates for in situ polymerization. J Anal Appl Pyrolysis 86:74–81